Journal of Magnetic Resonance **142,** 341–347 (2000)
doi:10.1006/jmre.1999.1947, available online at http://www.idealibrary.com on IDEAL®

Time-Domain Quantification of Multiple-Quantum-Filtered ^{23}Na Signal Using Continuous Wavelet Transform Analysis

Hacene Serrai,* Arijitt Borthakur,* Lotfi Senhadji,† Ravinder Reddy,* and Navin Bansal*

*Department of Radiology, University of Pennsylvania School of Medicine, Philadelphia, Pennsylvania 19104-6100; and †Laboratoire de Traitement du Signal et d'Images (LTSI), INSERM, Université de Rennes1, Campus de Beaulieu, 35042 Rennes, France

Received July 13, 1999

The application of continuous wavelet transform (CWT) analysis technique is presented to analyze multiple-quantum-filtered (MQF) ^{23}Na magnetic resonance spectroscopy (MRS) data. CWT acts on the free-induction-decay (FID) signal as a time-frequency variable filter. The signal-to-noise ratio (SNR) and frequency resolution of the output filter are locally increased. As a result, MQF equilibrium longitudinal magnetization and the apparent fast and slow transverse relaxation times are accurately estimated. A developed iterative algorithm based on frequency signal detection and components extraction, already proposed, was used to estimate the values of the signal parameters by analyzing simulated time-domain MQF signals and data from an agarose gel. The results obtained were compared to those obtained by measurement of signal height in frequency domain as a function of MQF preparation time and those obtained by a simple time-domain curve fitting. The comparison indicates that the CWT approach provides better results than the other tested methods that are generally used for MQF ^{23}Na MRS data analysis, especially when the SNR is low. The mean error on the estimated values of the amplitude signal and the apparent fast and slow transverse relaxation times for the simulated data were 2.19, 6.63, and 16.17% for CWT, signal height in frequency domain, and time-domain curve fitting methods, respectively. Another major advantage of the proposed technique is that it allows quantification of MQF ^{23}Na signal from a single FID and, thus, reduces the experiment time dramatically.

Key Words: **continuous wavelet transform; multiple-quantum-filtered ^{23}Na signal; magnetic resonance spectroscopy; quantification.**

1. INTRODUCTION

Multiple-quantum-filtered (MQF)[1] ^{23}Na magnetic resonance spectroscopy (MRS) has been proposed as a means to partially discriminate between intra- and extracellular Na^+ in tissue (*1*). The overwhelming advantage of multiple-quantum (MQ) filter techniques is that they allow noninvasive measurements and, thus, can be applied to humans. In general, some extracellular sodium signal also passes through a MQ filter (*2*); however, this signal is relatively insensitive to possible changes in extracellular sodium (*3, 4*). MQF ^{23}Na MRS has also been used to probe structural information in partially disordered biological systems such as cartilage (*5*). If this technique is to be of use in studies of intracellular Na^+ or for obtaining structural information, it must allow for accurate quantification of the observed MRS signal.

The MQF MRS signals can be recorded using the pulse sequence (*6*)

$$\pi/2-\tau/2-\pi-\tau/2-\pi/2-\delta-\pi/2-t_{\text{acq}},$$

where τ and δ are the MQ preparation and evolution time, respectively. The first part of this sequence is a standard spin-echo sequence. The second $\pi/2$ pulse creates the MQ coherences, which evolve during δ. The final $\pi/2$ pulse is the detection pulse, which transfers the coherence from the invisible MQ coherences to an observable single-quantum (SQ) coherence. Double-quantum (DQF)- or triple-quantum (TQF)-filtered signals are selected by appropriate phase cycling (*6*).

The collected MQF free induction decay (FID) is composed of two signal components, one from the inner transition and the other from the outer transitions. In an isotropic case (*6*), the inner and outer transitions have the same chemical shift and signal amplitude values but opposite phases and different time constants called apparent slow (T^*_{2s}) and fast (T^*_{2f}) transverse relaxation times, respectively. Thus the observed signal is a difference of two equal amplitude exponential functions. The amplitude of each MQF FID is also dependent on the preparation time τ and the relaxation times T_{2s} and T_{2f}. A biexponential function is thus the best model to represent the MQF ^{23}Na MRS signal in an isotropic case. However, the signal model becomes complicated in nonisotropic cases, such as cartilage (*7–9*), where the parameter representing the quadrupolar splitting interaction must be included in the signal model.

The most commonly used method for quantification of MQF ^{23}Na signal is based on measurement of signal height in frequency domain (*10*). It requires acquisition of a number of

[1] Abbreviations used: MQF, multiple-quantum filtered; TQF, triple-quantum filtered; DQF, double-quantum filtered; SQ, single quantum; MQ, multiple quantum; MR, magnetic resonance; MRS, magnetic resonance spectroscopy; CWT, continuous wavelet transform; MPH, maximum peak height; SNR, signal-to-noise ratio; FID, free induction decay.

1090-7807/00 $35.00

MQF FIDs at different τ values. The MQF FIDs are then Fourier transformed and the spectral maxima are fit to a biexponential function to estimate the MQF equilibrium longitudinal magnetization (M_0), T_{2s}, and T_{2f}. We will refer to this method as the maximum peak height (MPH) method. A major drawback of this method is that it requires a long experiment time because several MQF FIDs at different τ values have to be collected. The other possible technique to quantify MQF ^{23}Na signal is a classical time-domain curve fitting method. This method can be used to quantify MQF signal from a single FID and, thus, it does not suffer from the long experiment time. A similar approach may be used in the frequency domain. However, these methods do not perform well at low signal-to-noise ratio (SNR).

We propose the use of the wavelet transform method to analyze MQF ^{23}Na signal. Wavelet transform has found applications in a number of disciplines including MRS (*11, 12*). The advantage of wavelet transform is due to the fact it can be used to approximate signals according to scale resolution using a set of prototype functions called wavelets. It allows representation of the original data in a two-dimensional plane in which both frequency and time information are retained. The continuous form of the transform (CWT) was proposed as a quantification method in MRS signal processing. It has been successfully tested for quantification of ^{1}H and ^{31}P MRS time-domain data (*13*) and for analysis of solid-state ^{13}C MRS signals (*14*). It has also been used to eliminate the solvent peak in unsuppressed ^{1}H MRS data and to compensate for eddy-currents artifacts (*15*). In this paper, we have used the same approach as in Refs. (*13*) and (*14*) for quantification of MQF ^{23}Na signal.

The objectives of this study were (1) to evaluate the ability of CWT analysis in estimating M_0, T_{2f}^*, and T_{2s}^* values in the absence of residual quadrupolar splitting, from a single time-domain MQ-filtered ^{23}Na MRS signal while effectively reducing the experiment time; and (2) to determine whether CWT analysis provides better results compared to previously used MQ-filtered data analysis methods, especially when the SNR is low.

2. THE CONTINUOUS WAVELET TRANSFORM IN MRS SIGNAL PROCESSING

CWT analyzes a nonstationary signal by transforming its input time domain into a time-scale domain (*16*). Through translation and dilation operations, CWT decomposes the signal according to a set of functions deduced from a defined prototype function, assumed to be well localized in both time and frequency domains.

In mathematical terms, CWT of a signal $s(t)$ of a finite energy with respect to a prototype function $g(t)$ in the time domain is given by

$$S_a(b) = < s, g_{a,b} > = \frac{1}{a} \int s(t)\, g_{a,b}{}^{*}\left(\frac{t-b}{a}\right) dt, \quad [1]$$

with $g_{a,b}(t) = (1/a)\, g((t-b)/a)$, characterized by two parameters, the scale or dilation parameter noted a ($a > 0$) and the translation parameter noted b ($b \in R$). The asterisk stands for the complex conjugate.

In the Fourier domain, Expression [1] takes the form

$$S_a(b) = \frac{1}{2\pi} \int \hat{s}(\omega)\, \hat{g}_{a,b}{}^{*}(a\omega) e^{i\omega b} d\omega, \quad [2]$$

where $\hat{s}$ and $\hat{g}$ are the Fourier transforms of the signal s and of the wavelet g.

Any prototype function $g(t)$ belonging to $L^2(R)$ is called an analyzing wavelet if it complies with the so-called admissibility condition (*17*). The transform in Eq. [1] maps the signal via a two-dimensional function $S_a(b)$ on the time-scale domain plane (a, b). This operation is equivalent to a particular filter-bank analysis in which the relative frequency bandwidths ($\Delta\omega/\omega$) are constant and related to the parameters a, b and to the frequency properties of the wavelet g.

Consider $s(t)$ a noiseless MRS time-domain signal composed of one damped complex sinusoid decaying with time, given by

$$s(t) = A \exp\left(\frac{-t}{T_2^*}\right) \exp(i(\omega_s t + \varphi)), \quad [3]$$

where A, T_2^*, ω_s, and φ are the resonance amplitude, apparent relaxation time, angular frequency, and phase, respectively.

To achieve a correct analysis of the signal $s(t)$, regularity and suitable time-frequency bandwidth product are required for g. The most commonly used analyzing wavelet has been the so-called Morlet wavelet written as (*16, 17*)

$$g(t) = \exp\left(\frac{-t^2}{2}\right) \exp(i\omega_0 t) + c(t), \quad [4]$$

where $c(t)$ is a correction term to enforce the admissibility condition. For $\omega_0 > 5$, the term $c(t)$ is numerically negligible and $g(t)$ is practically applicable. One can check this property by taking the Fourier transform of g,

$$\hat{g}(\omega) = \sqrt{2\pi} \exp\left(\frac{-(\omega-\omega_0)^2}{2}\right) + \hat{c}(\omega), \quad [5]$$

which approaches to zero when $\omega \leq 0$ (*18*). The term $\hat{c}(\omega)$ is the Fourier transform of $c(t)$. The Morlet wavelet can be seen as a bandpass filter centered at $\omega = \omega_0/a$ weighted by the factor $1/a$. Due to the causality of the MQF ^{23}Na MRS signals ($s(t) \in R^+$), our conventions (a, $b \in R^+ \times R^+$) for the time-frequency display are the same as in Ref. (*11*).

Substituting $s(t)$ and $g(t)$ for Eqs. [3] and [4], respectively, in Eq. [1] and referring to (*13*), the CWT of $s(t)$ is given by

$$S_{a_r}(b) = \sqrt{\frac{\pi}{2}} A\left[\exp\left(\frac{a_r^2 - 2bT_2^*}{2T_2^{*2}}\right)\right] \times [1 \mp \sqrt{1-\exp(-\alpha)^2}]\exp(i(\omega_s b + \varphi)), \quad [6]$$

where a_r is the final dilation parameter value obtained at the convergence of the used iterative algorithm (*13*), with $\alpha = [(a_r/T_2^*) - (b/a_r)]$ and the signs $\mp$ are conditioned by the sign of α.

A simple nonlinear regression algorithm (*19*) applied on the modulus of the above equation gives the values of A and T_2^*, whereas the angular frequency ω_s and phase φ are linearly estimated from the phase of $S_{a_r}(b)$.

Now, consider a noiseless MQF ^{23}Na signal obtained using a constant preparation time τ and a negligibly small evolution time δ in the absence of the residual quadrupolar splitting interaction. It is given by (*6*)

$$s(t,\tau) = A(\tau)\left[\exp\left(\frac{-t}{T_{2s}^*}\right) - \exp\left(\frac{-t}{T_{2f}^*}\right)\right]\exp(i(\omega_s t + \varphi)), \quad [7]$$

where

$$A(\tau) = M_0 K_{MQ}\left[\exp\left(\frac{-\tau}{T_{2s}}\right) - \exp\left(\frac{-\tau}{T_{2f}}\right)\right]. \quad [8]$$

K_{MQ} is a constant equal to 3/20 for DQF ^{23}Na signal and 9/40 for TQF ^{23}Na signal (*6*).

Using the same procedure as described in Ref. (*13*) and following the above steps, the CWT of $s(t, \tau)$ is given by

$$S_{a_r}(b,\tau) = A(\tau)\sqrt{\frac{\pi}{2}}\left[\left[\exp\left(\frac{a_r^2 - 2bT_{2s}^*}{2T_{2s}^{*2}}\right)\right] \times [1 \mp \sqrt{1 - \exp(-\alpha_1)^2}] - \left[\exp\left(\frac{a_r^2 - 2bT_{2f}^*}{2T_{2f}^{*2}}\right)\right] \times [1 \mp \sqrt{1 - \exp(-\alpha_2)^2}]\right]\exp(i(\omega_s + \varphi)), \quad [9]$$

where $\alpha_1 = [(a_r/T_{2s}^*) - (b/a_r)]$ and $\alpha_2 = [(a_r/T_{2f}^*) - (b/a_r)]$. The values of $A(\tau)$, T_{2s}^*, and T_{2f}^* are nonlinearly estimated from the modulus of Eq. [9]. Substituting T_{2s} and T_{2f} for T_{2s}^*, T_{2f}^* values in Eq. [8], the value of M_0 is recovered. The values of ω_s and φ are linearly estimated from the phase of $S_{a_r}(b, \tau)$.

In the real case, the MQF ^{23}Na MRS signals are collected with noncorrelated random noise. In order to analyze the data accurately, the noise contribution should be reduced in the result of $S_{a_r}(b, \tau)$. Both ω_0 and a_r values have to be increased by the same factor f. The central frequency of the wavelet is held focused on the signal frequency $\omega_s = (f \cdot \omega_0)/a_r$. This effectively reduces the bandwidth ($\Delta\omega/\omega$) of the filter. The shape of the signal recovered from the output filter approaches to Eq. [9] (*13, 15*).

Starting values are required for the analyzing frequency ω_0, translation parameter b, and dilation parameter a of the Morlet wavelet when running the iterative algorithm described in Refs. (*13*) and (*14*).

3. MATERIAL AND METHODS

The accuracy and the efficiency of the proposed CWT analysis were evaluated on MQF ^{23}Na simulated signal and data from an agarose gel. The results obtained were compared to those obtained by time-domain curve fitting and MPH technique. The biexponential model was used in all the methods to analyze the MQF ^{23}Na MRS data.

For CWT analysis, the iterative procedure described in (*13*) was used for each MQF ^{23}Na MRS signal. The starting value of the analyzing frequency ω_0 of the wavelet was set to 10 so that the admissibility condition is satisfied. The initial value of the dilation parameter a was taken as 1. Because both of the signal components of the MQF ^{23}Na FID decay with the same frequency, the value of translation parameter b was fixed to 12 for all the FIDs (see Ref. *13* for more details). Equation [9] was used in estimating the values of T_{2s}^*, T_{2f}^*, and $A(\tau)$, and Eq. [8] was used to obtain the M_0 value.

For the time-domain curve fitting, each FID signal was first phase corrected such that the imaginary part of the signal only contained noise. The real part of the signal was then fit to Eq. [7] to estimate the values of $A(\tau)$, T_{2s}^*, and T_{2f}^*. The value of M_0 for each signal FID was calculated using Eq. [8].

For the MPH method, the MQF FIDs were Fourier transformed and the signal maxima for various τ values were fit to

$$\text{PeakHeight} = A_0\left[\exp\left(\frac{-\tau}{T_{2s}}\right) - \exp\left(\frac{-\tau}{T_{2f}}\right)\right]. \quad [10]$$

The value of M_0 was determined using the relation

$$M_0 = \frac{A_0}{K_{MQ}(T_{2s}^* - T_{2f}^*)}. \quad [11]$$

The three tested procedures for the analysis of MQF ^{23}Na signal were implemented in Interactive Data Language (IDL) (Research Systems, Inc., Boulder, CO).

Synthetic data. Synthetic MQF ^{23}Na MRS FIDs based on the biexponential model of Eq. [7] with a randomly uniform added noise were generated using a program written in IDL. $A(\tau)$ was substituted for Eq. [8] in Eq. [7]. The sampling frequency was set to 10 kHz and 1024 complex data points

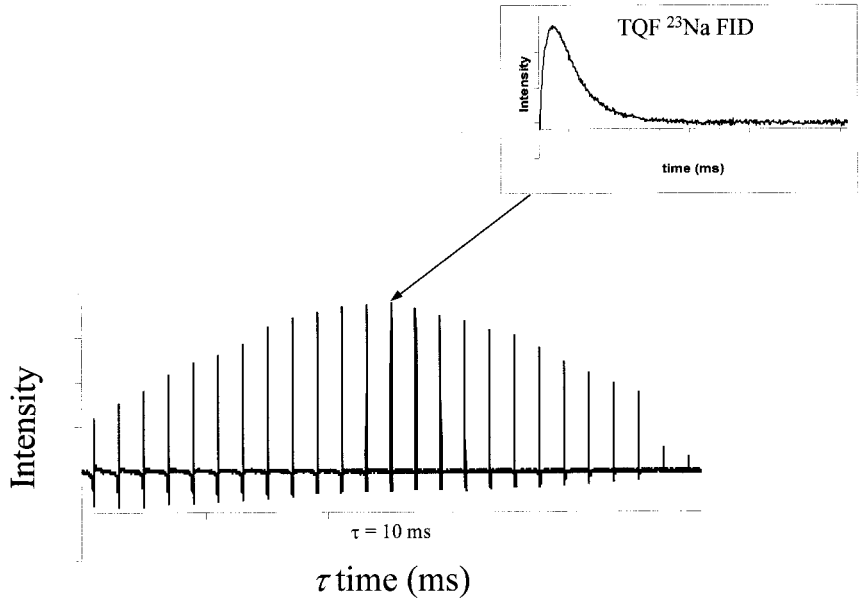

FIG. 1. Variation of MQF ^{23}Na MRS signal intensity as a function of preparation time τ in the agarose gel sample. The inset is the corresponding time-domain FID at optimum $\tau = 10$ ms.

were used to simulate each FID. The value of M_0K_{MQ} was set to 100 arbitrary units (au). Fourteen different values of τ ranging from 0.5 to 40 ms were used to synthesize 14 FIDs for a given MQF data set. First the effect of changing the SNR was evaluated. For this purpose, three different MQF data sets, each containing 14 FIDs, were generated with white noise levels of 1 au and SNR ranging from 17 to 33 dB and 10 au and SNR ranging from 1 to 11 dB and 20 au and SNR ranging from 0 to 5 dB. The values of T^*_{2f} and T^*_{2s}were set to 2 and 18 ms, respectively. Second, the effects of varying the T^*_{2f} while keeping T^*_{2s} equal to 18 ms with the three noise levels were investigated. For noise level of 1 au, the SNR is ranged from 6 to 29 dB. For noise level equal 10 au, the SNR varies from 1 to 7 dB and for noise level equal 20 au, the SNR changes from 0 to 2 dB. T^*_{2f} was set to 1, 2, and 4 ms. Last, the effects of changing T^*_{2s} while T^*_{2f} was held equal to 2 ms were studied at the same three noise levels. T^*_{2s} was set to 16, 18, and 20 ms. The corresponding SNR values range from 14 to 29 dB for noise level of 1 au, from 0 to 8 dB for noise level of 10 au, and from 0 to 2 dB for noise level of 20 au.

TQF ^{23}Na signal from agarose gel. An agarose gel sample was prepared by dissolving 6% agarose in a 300 mM NaCl solution with mild heating followed by cooling the sample to room temperature. TQF ^{23}Na MRS data from the gel sample were obtained at 400 MHz on a vertical bore spectrometer (Bruker Instruments, Billerica, MA) using the pulse sequence described in the introduction. The acquisition parameters were 384 accumulations, $\pm$2500 Hz spectral width, 512 data points, and 250 ms repetition time. Twenty-eight FIDs were collected using different τ values ranging from 0.4 to 80 ms. The evolution time δ was kept as short as possible (10 μs) to allow a phase change between the last two radiofrequency pulses. Both MPH and CWT methods were used to analyze the data (Fig. 1).

4. RESULTS

Synthetic data. In the first test, the efficiency of CWT analysis when the SNR is low was evaluated. The results reported in Table 1 show that CWT provides more accurate results, with low noise levels, for the signal parameters, especially the M_0K_{MQ} value, than those obtained by time-domain curve fitting or MPH method. As shown in Fig. 2, time-domain curve fitting overestimates M_0K_{MQ} values, whereas CWT is more reliable. This is achieved by shortening the support length (frequency bandwidth) of the wavelet in the frequency domain; only the signal frequency passes through. The signal is thus isolated from noise. As a consequence, the M_0K_{MQ} value is accurately estimated.

The effects of varying T^*_{2f} with different noise levels were considered in the second test. The results obtained show that CWT analysis provides better results in estimating this parameter than time-domain curve fitting (Table 2). Because the fast component of the MQF ^{23}Na signal decays very rapidly with time, the data resolution is poor in the beginning of the signal. CWT is more reliable in estimating the T^*_{2f} than time-domain curve fitting, which gave less accurate results even with high SNR.

In the last test, the effect of varying T^*_{2s}, and SNR was evaluated. The results reported in Table 3 show that CWT analysis provides better results than both the time-domain curve fitting and the MPH method, especially with low SNR.

TABLE 1

Estimated Values of the MQF MRS Parameters Obtained by CWT, MPH, and Time-Domain Curve Fitting of the Simulated Data Sets with Three Different Noise Levels

	Actual values	MPH	Time-domain curve fitting	CWT
Noise level = 1				
A (au)	100	106.9	102 ± 4	100.1 ± 0.3
T^*_{2f} (ms)	2	2.1	1.97 ± .02	2.01 ± .01
T^*_{2s} (ms)	18	16.7*	17.5 ± 0.1	17.9 ± .07
Noise level = 10				
A (au)	100	97.8	89 ± 3*	98.3 ± 2.0
T^*_{2f} (ms)	2	2.0	1.36 ± .09*	1.99 ± .06
T^*_{2s} (ms)	18	17.8	17.5 ± 1.0	18.2 ± 0.3
Noise level = 20				
A (au)	100	97.5	114.5 ± 19*	101. ± 1.1
T^*_{2f} (ms)	2	2.1	2.36 ± 0.21	2.1 ± 0.1
T^*_{2s} (ms)	18	17.1	18.4 ± 3.40	18.3 ± 0.4

Note. Each MQF MRS data set contains 14 FIDs. The results obtained by CWT and time-domain curve fitting are the mean value ± standard deviation (SD). For comparison, the estimated values of T^*_{2f} and T^*_{2s} are also reported in Tables 2 and 3, respectively. The asterisk indicates that the estimated parameter values are significantly different than the expected ones.

Both the time-domain curve fitting and the MPH method appear to be disturbed by the SNR factor.

TQF ^{23}Na signal from agarose gel. To further demonstrate the usefulness of the CWT as a TQF ^{23}Na MRS quantification technique, we have analyzed data from an agarose gel sample and compared the results to those obtained by the MPH method. CWT analysis and the MPH method provided similar results (Table 4). The SNR values for the first acquired FID, the one at optimum τ (τ = 10 ms), and the last FID are 29, 35, and 14 dB, respectively. The small differences in the estimated relaxation times values could be explained by the fact that CWT analysis estimates the apparent relaxation time values whereas MPH provides the values of T_{2s} and T_{2f}. The fast relaxation time is less sensitive to field inhomogeneity effects than the slow one. The difference in the estimated T_{2f} values is more related to the efficiency of the methods. As shown above, CWT is more reliable in estimating this parameter than MPH method. The estimation of T_{2s} is more affected by the field inhomogeneity when using CWT, which provides the broadened form of T_{2s}, e.g., T^*_{2s}value.

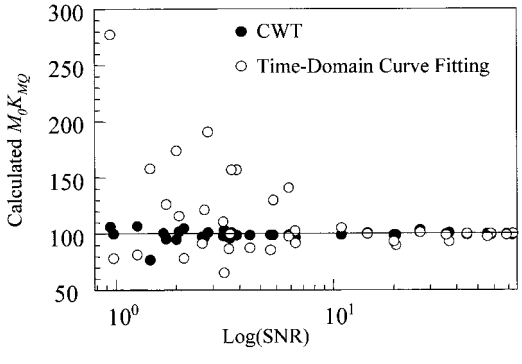

FIG. 2. Comparison between time-domain curve fitting and CWT analysis for calculation of M_0K_{MQ} at different noise levels for synthetic data.

TABLE 2

Estimated T^*_{2f} Values Obtained by CWT, MPH, and Time-Domain Curve Fitting from Simulated MQF MRS Data with Three Different Noise Levels

Noise level	Actual value (ms)	MPH	Time-domain curve fitting	CWT
1	1	1.1	1.2 ± .03	1.0 ± .02
10	1	1.1	0.4 ± .04*	1.0 ± .01
20	1	0.9	1.9 ± 0.2*	1.1 ± .08
1	2	2.1	1.9 ± .02	2.0 ± .01
10	2	2.0	1.4 ± 0.1*	1.9 ± .06
20	2	2.1	2.4 ± 0.2	2.1 ± 0.1
1	4	4.2	4.2 ± .02	4.0 ± .01
10	4	4.1	3.5 ± 0.2*	3.9 ± .01
20	4	4.5*	3.2 ± 0.1*	3.9 ± .07

Note. The values of A and T^*_{2s} are 100 au and 18 ms, respectively. Each data set contains 14 FIDs. Both CWT and time-domain curve fitting estimate the parameter values from a single FID. Their shown results are the mean value ± SD. The asterisk indicates that the estimated parameter values are not close to the expected ones.

5. DISCUSSION

A technique based on CWT analysis has been proposed for the analysis of MQF ^{23}Na data. Using the same procedure as in (*13*), CWT is able to extract the signal information without any

TABLE 3

Estimated T^*_{2s} Values Obtained by CWT, MPH, and Time-Domain Curve Fitting from Simulated MQF MRS Data with Three Different Noise Levels

Noise level	Actual value (ms)	MPH	Time-domain curve fitting	CWT
1	16	14.8*	14.7 ± 0.1*	15.9 ± 0.1
10	16	15.8	15.1 ± 0.4	16.4 ± 0.1
20	16	23.0*	10.0 ± 0.6*	17.0 ± 0.2
1	18	16.9	17.5 ± 0.1	17.9 ± .07
10	18	17.8	17.5 ± 1.0	18.2 ± 0.3
20	18	17.1	18.4 ± 3.4	18.3 ± 0.4
1	20	18.5	18.6 ± 0.1	19.8 ± .05
10	20	19.8	20.1 ± 0.3	19.4 ± .03
20	20	17.8	15.8 ± 1.1*	18.9 ± 0.1

Note. The values of A and T^*_{2f} are 100 au and 2 ms, respectively. Each analyzed data set contains 14 FIDs. The results shown from CWT and time-domain curve fitting are the mean value ± SD of the 14 FIDs. The asterisk indicates that the estimated parameter values are significantly different from the actual ones.

TABLE 4
Comparison of the Results Obtained by CWT and MPH Analysis from a Set of Agarose Gel TQF ^{23}Na MRS Data

T^*_{2f} (ms)		T^*_{2s} (ms)		M_0 (au)	
MPH (T_{2f})	CWT	MPH (T_{2s})	CWT	MPH	CWT
5.53	5.90 ± .03	26.45	22.49 ± .001	179033	186509 ± 220

Note. MPH method estimates T_{2f} and T_{2s} values, whereas CWT calculates the values of T^*_{2f} and T^*_{2s}. The results obtained by CWT from 28 FIDs are the mean value ± standard deviation.

prior knowledge of the signal parameters to be determined. Compared to time-domain curve fitting and the MPH method, CWT analysis appears efficient in obtaining accurate estimates of the values of the MQF ^{23}Na signal parameters: M_0, T^*_{2s}, and T^*_{2f}.

The low SNR may affect the accuracy of the obtained results. By shortening the support length of the wavelet in the frequency domain, the noise contribution in the data is reduced accordingly. Thus, the method provides better results at low SNR than the time-domain curve fitting method.

The effect of poor signal resolution on the parameter estimation has been verified. The obtained results on both of the apparent relaxation times demonstrate that CWT is less affected by the signal resolution than time-domain curve fitting and the MPH method.

The MPH method is the most commonly used technique in MQF ^{23}Na MRS signal processing. It allows an estimation of T_{2f} and T_{2s} values. Noise filtering by using line broadening may increase the SNR and improve the accuracy of the results obtained by the MPH technique. However, its major drawback is the long experiment time. CWT provides similar results by processing only one single MQF ^{23}Na MRS signal. Data collection time is then considerably reduced. This represents a major advantage for applications of MQF ^{23}Na MRS technique to humans. Furthermore, phase corrections and line broadening are not required with CWT analysis.

6. CONCLUSION

In summary, we demonstrate that CWT analysis provides better quantification of MQF ^{23}Na MRS signal than the MPH method and time-domain curve fitting, especially when the SNR is low. Another major advantage of CWT analysis is that it allows quantification of the MQF signal from a single FID and, thus, reduces the experiment time dramatically. The analysis data from the agarose gel sample demonstrate that the CWT analysis is suitable for analyzing MQF ^{23}Na MRS signal from real samples in the absence of residual quadrupolar splitting. Further work is in progress to apply the CWT technique for the analysis of *in vitro* and *in vivo* MQF signals and in the presence of quadrupolar splitting in biological tissues.

ACKNOWLEDGMENTS

This work was supported in part by Grants HL-54574 (NB) and AR45242 (RR) from the National Institutes of Health and by a grant from the Whitaker Foundation (NB). A part of this work was presented at the Seventh Scientific Meeting and Exhibition of ISMRM, May 22–28, 1999, Philadelphia, PA.

REFERENCES

1. J. Pekar, P. F. Renshaw, and J. S. Leigh, Selective selection of intracellular sodium by coherence-transfer NMR, *J. Magn. Reson.* **72,** 159–161 (1987).
2. L. A. Jelicks and R. K. Gupta, Multinuclear NMR studies of the Langendorff perfused rat heart, *J. Biol. Chem.* **264,** 15230–15235 (1989).
3. V. Seshan, A. D. Sherry, and N. Bansal, Evaluation of triple quantum-filtered ^{23}Na imaging of rabbit kidney with weighted signal averaging, *Magn. Reson. Med.* **38,** 821–827 (1997).
4. V. D. Schepkin, I. O. Choy, T. F. Budinger, D. Y. Obayashi, S. E. Taylor, W. M. De Campli, S. C. Amartur, and J. N. Young, Sodium TQF NMR and intracellular sodium in isolated crystalloid perfused rat heart, *Magn. Reson. Med.* **39,** 557–563 (1998).
5. U. Eliav, H. Shinar, and G. Navon, The formation of a second-rank tensor in ^{23}Na double-quantum-filtered NMR as an indicator for order in biological tissue, *J. Magn. Reson.* **98,** 223–229 (1992).
6. V. Seshan and N. Bansal, *in* "NMR Spectroscopy Techniques" (M. D. Bruch, Ed.) p. 589, Dekker, New York (1996).
7. R. Reddy, L. Bolinger, M. Shinnar, E. Noyszewski, and J. S. Leigh, Detection of residual quadrupolar interaction in human skeletal muscle and brain in-vivo via multiple quantum filtered sodium NMR spectra, *Magn. Reson. Med.* **33,** 134–139 (1995).
8. U. Eliav and G. Navon, Analysis of double-quantum-filtered NMR spectra of ^{23}Na biological tissues, *J. Magn. Reson. B* **103,** 19–29 (1994).
9. H. Shinar, U. Eliav, T. Knubovetz, Y. Sharf, and G. Navon, Measurement of order in connective tissues by multiple quantum filtered NMR spectroscopy of quadrupolar nuclei, *Q. Magn. Reson. Biol. Med.* **2,** 73–82 (1995).
10. J. Whang, J. Katz, L. M. Boxt, K. Reagan, D. J. Sorce, R. R. Sciacca, and P. J. Cannon, Multiple-quantum-filtered NMR determination of equilibrium magnetization for ^{23}Na quantitation in model phantoms, *J. Magn. Reson. B* **103,** 175–179 (1994).
11. N. Delprat, B. Escudie, Ph. Guillemain, R. Kronland-Martinet, Ph. Tchamitchian, and B. Torresani, Asymptotic wavelet and Gabor analysis: Extraction of instantaneous frequencies, *IEEE Trans. Inform. Theory* **38,** 644–664 (1992).
12. G. Neue, Simplification of dynamical NMR spectroscopy by wavelet transform, *Solid State Nucl. Magn. Reson.* **5,** 305–314 (1996).
13. H. Serrai, L. Senhadji, J. D. de Certaines, and J-L. Coatrieux, Time-domain quantification of amplitude, chemical shift, apparent relaxation time T^*_2, and phase by wavelet-transform analysis. Application to biomedical magnetic resonance spectroscopy, *J. Magn. Reson.* **124,** 20–34 (1997).
14. H. Serrai, L. Nadal, M. Le Floch, G. Leray, L. Senhadji, N. Le Tallec, and J. D. de Certaines, Wavelet transform in magnetic resonance data processing: Application to subtraction of broad resonances,

resolution of overlapping peaks and quantification, *J. Magn. Reson. Anal.* **3,** 79–86 (1997).

15. D. Barache, J-P. Antoine, and J-M. Dereppe, The continuous wavelet transform, an analysis tool for NMR spectroscopy, *J. Magn. Reson.* **128,** 1–11 (1997).

16. A. Grossmann and J. Morlet, Decomposition of hardy functions into square integrable wavelets of constant shape, *SIAM J. Math. Anal.* **15,** 723–736 (1984).

17. A. Grossmann, R. Kronland-Martinet, and J. Morlet, *in* "Wavelets" (J. M. Combes, A. Grossmann, and Ph. Tchamitchian, Eds.), p. 1, Springer Verlag, Marseille (1987).

18. Ph. Guillemain, R. Kronland-Martinet, and B. Martens, *in* "Wavelets and Applications" (Y. Meyer, Ed.), p. 39, Masson, Marseille (1989).

19. D. W. Marquardt, An algorithm for least-squares estimation of nonlinear parameters, *J. Soc. Indust. Appl. Math.* **11,** 431–441 (1963).

20. J. Andrasko, Nonexponential relaxation of ^{23}Na in agarose gels, *J. Magn. Reson.* **16,** 502–504 (1974).